Ho *et al. Chem. Biol. Technol. Agric.* (2023) 10:47
https://doi.org/10.1186/s40538-023-00427-2

Chemical and Biological Technologies in Agriculture

RESEARCH

Open Access

Structural characterization of water-soluble polysaccharides isolated from leaves of *Hedera nepalensis*

ChungHyok Ho[1], Yuwen Wang[1], Xianbin Liu[1], Yifa Zhou[1], UnHak Pak[1*] and Lin Sun[1*]

Abstract

Background *Hedera nepalensis* is a traditional medicinal plants, and the dried leaves of it are generally used for the cure and treatment of many diseases, also widely known as Chang-Chun-Teng in Chinese. Until now, structural characterization of water-soluble polysaccharides isolated from leaves of *Hedera nepalensis* have been scarcely studied, even though the chemical compounds derived from it and their biological activities have been widely studied.

Methods Water-soluble polysaccharides (WHNP) were isolated from the dried leaves of *Hedera nepalensis*, and their structural features were investigated. One neutral polysaccharide fraction (WHNP-N) and three major pectin fractions (WHNP-A2b, WHNP-A2c and WHNP-A3b) were obtained from WHNP, respectively. There was no analysis of the neutral fraction (WHNP-N), while the structural characterization of three major pectin fractions (WHNP-A2b, WHNP-A2c and WHNP-A3b) were further studied by monosaccharide composition, HPGPC, NMR and methylation analyses.

Results The results indicated that two fractions WHNP-A2b (Mw = 45.8 kDa) and WHNP-A3b (Mw = 58.6 kDa) were mainly composed of rhamnogalacturonan I (RG-I). In WHNP-A2b, RG-I domains primarily substituted with α-L-1,5/1,3,5-arabinan, type II arabinogalactan (AG-II), β-D-1,4-galactan and/or type I arabinogalactan (AG-I) as side chains, while RG-I-type pectin of WHNP-A3b mainly branched with α-L-1,5/1,3,5-arabinan, β-D-1,4-galactan and AG-II side chains. WHNP-A2c (Mw = 12.4 kDa) was primarily comprised of galacturonic acid (GalA, 60.8%), and enzymatic analysis indicated that this fraction mainly consisted of rhamnogalacturonan I (RG-I), rhamnogalacturonan II (RG-II) and homogalacturonan (HG) domains with mass ratios of 1.8:1.0:0.6. On the other hand, WHNP-A2c was found to be rich in RG-I domains, which contained α-L-1,5/1,3,5-arabinan, AG-II, β-D-1,4-galactan and/or AG-I as side chains. The HG domains of WHNP-A2c was released in the form of un-esterified and partly methyl-esterified and/or acetyl-esterified oligogalacturonides with a 1 to 7 degree of polymerization after endo-polygalacturonase degradation.

Conclusion Our results reveal the structural characteristics of these polysaccharide fractions, which will contribute to elucidating their structure–activity relationships.

Keywords *Hedera nepalensis*, Pectin, Polysaccharides, Endo-polygalacturonase, Structural characterization

*Correspondence:
UnHak Pak
piaoex070@nenu.edu.cn
Lin Sun
sunl925@nenu.edu.cn
Full list of author information is available at the end of the article

Graphical Abstract

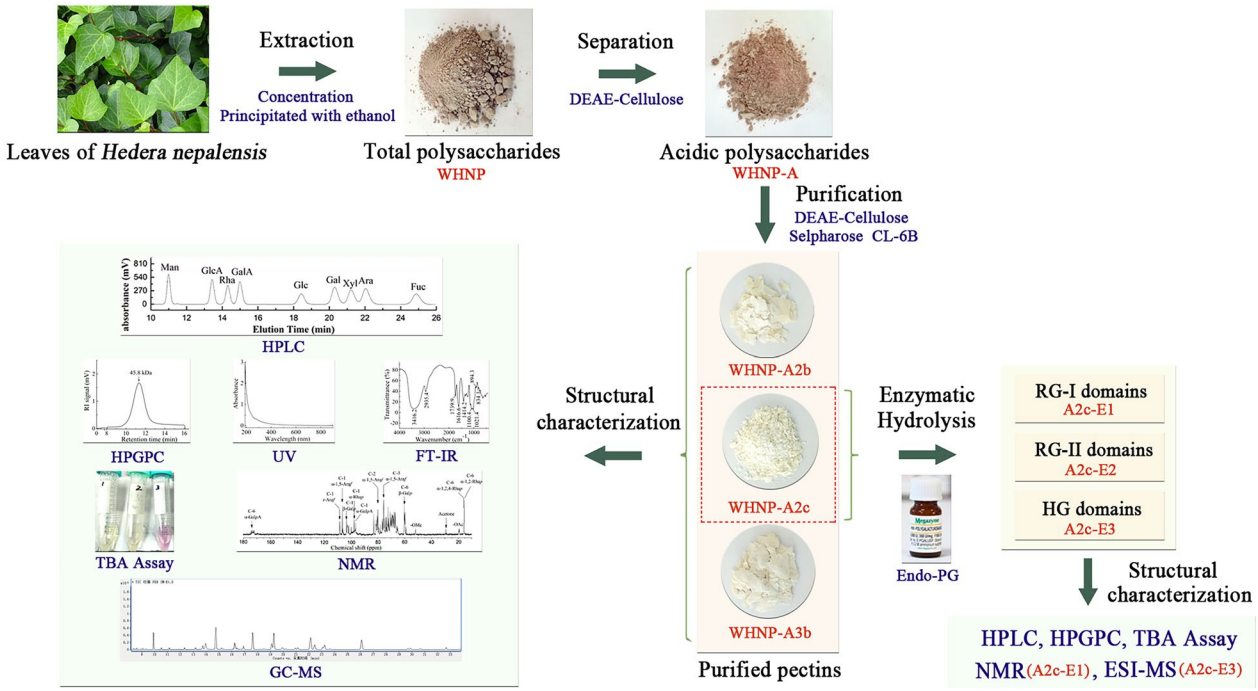

Introduction

Hedera nepalensis is widely used in traditional Chinese medicines, which belongs to the family of *Araliaceae*, and is called "Chang Chun Teng" in Chinese. It is widely cultivated as an ornamental vine in eastern Asia, and has long been used as a herbal medicine for the treatment of diabetes, cancer, etc. [1–5]. Also, *Hedera nepalensis* is a recognized medicinal plant that has been reported to work in antifungal, antimicrobial, antioxidant and antitumor capacities [6–10].

Many researchers have paid attention to the phytochemicals obtained from *Hedera nepalensis* in the relation to their isolation, purification, and characterization [1–11]. Kizu et al. isolated various chemical compounds consisting of a complex mixture of saponins from *Hedera nepalensis* for the first time [11]. Saleem et al. reported that the extracts of *Hedera nepalensis* contained the triterpenoid lupeol with significant dipeptidyl peptidase-4 (DPP-4) inhibitory activity [1]. Li et al. isolated and identified two anticancer compounds (pulsatilla saponin A and hederagenin 3-O-α-L-arabinopyranoside) from the 95% ethanol extract of *Hedera nepalensis* [7]. Jafri et al. reported this plant contains plenty of phenol chemical compounds, which show significant antioxidant potential [9]. Duong et al. mentioned a model, which provides a robust experimental process for optimizing the extraction factors of saponin contents from *Hedera nepalensis* extract using subcritical fluid extraction and response surface methodology (RSM) [10]. Besides, the phytochemical analysis of *Hedera nepalensis* showed the presence of various chemical compounds such as alkaloids, glycosides, flavonoids, steroids, tannins and terpenoids [1–11].

Polysaccharides are the bioactive components of medicinal plants and have a lot of bioactivities. Pectins are categorized as acidic polysaccharides because of their high levels of uronic acid residues, and possess various activities, including immunological regulation, anti-cancer, hypoglycemic effect, antiviral activity and anti-inflammatory effect [12–15]. However, despite extensive research on the chemical compounds derived from *Hedera nepalensis* and their biological activities, the study of polysaccharides from this plant has been limited [1–11].

So, in this study, we isolated the total fractions of water-soluble polysaccharides from the leaves of *Hedera nepalensis* and conducted a detailed analysis of their structural features. The results are expected to have great significance in further investigating the

structure–activity relationships of the water-soluble polysaccharides from *Hedera nepalensis*.

Materials and methods

Materials and reagents

The dried leaves of *Hedera nepalensis* were purchased from Jiangxi province of China. DEAE-Cellulose was purchased from Shanghai Chemical Reagent Research Institute (Shanghai, China). Sepharose CL-6B and Sephadex G-75 were provided by GE Healthcare (Pittsburgh, USA). The enzyme endo-polygalacturonase (Endo-PG, E.C.3.2.1.15) was purchased from Megazyme (Bray, Ireland). All other reagents and chemicals were of analytical grade and bought from China.

General methods

Total carbohydrate content was determined using the phenol–sulphuric acid protocol [16]. Uronic acid content was measured by employing the m-hydroxydiphenyl method [17]. Monosaccharide composition analysis was conducted through PMP pre-column derivatization and HPLC detection [18]. In brief, 2 mg of sample was first hydrolyzed using anhydrous methanol containing 2 M HCl at 80 °C for 16 h and then with 2 M TFA at 120 °C for 1 h. Released monosaccharides were derived by using 1-phenyl-3-methyl-5-pyrazolone (PMP) and analyzed by HPLC on a DIKMA Inertsil ODS-3 column (4.6 mm × 150 mm) connected to a Shimadzu HPLC system (LC-20ATvp pump and UV detector, Shimadzu, Tokyo, Japan). Anion-exchange and size-exclusion chromatographies were monitored by assaying the total sugar and uronic acid content. Molecular weights (Mw) were determined using high performance size-exclusion chromatography (HPSEC) on a TSK-gel G-3000 PWXL column (7.8 × 300 mm, TOSOH, Tokyo, Japan) pre-calibrated by using standard dextrans (50 kDa, 25 kDa, 12 kDa, 5 kDa, 1 kDa, 666 Da, 342 Da and 180 Da) or TSK-gel G-4000 PWXL column (7.8 × 300 mm, TOSOH, Tokyo, Japan) pre-calibrated by using standard dextrans (670 kDa, 410 kDa, 270 kDa, 150 kDa, 80 kDa, 50 kDa, 25 kDa, and 12 kDa), coupled to a Shimadzu HPLC system (Tokyo, Japan) [18]. RG-II was qualitatively determined by adopting the modified thiobarbituric acid (TBA) assay [19].

Extraction of water-soluble polysaccharides

The dried leaves of *Hedera nepalensis* (1 kg) were extracted in 16 L distilled water at 100 °C for 6 h, which were filtered. After that, the procedures described above were repeated twice under identical conditions. The filtrates were combined, concentrated under vacuum at 60 °C, and centrifuged at 4500 rpm for 20 min to remove water-insoluble materials. The supernatant was precipitated overnight by adding 95% ethanol (4 volumes). The precipitates were centrifuged and dried using 95% ethanol and absolute ethanol, resulting in crude polysaccharides. Consequently, water-soluble *Hedera nepalensis* polysaccharides were obtained, referred to as WHNP.

Fractionation of water-soluble polysaccharides

WHNP was dissolved in distilled water and loaded onto a DEAE-Cellulose column (Cl^-, 8.0 cm × 20 cm). It was then eluted stepwise with H_2O and 0.5 M NaCl to obtain the neutral fraction WHNP-N and acidic fraction WHNP-A, respectively. WHNP-A was further applied to an analytical DEAE-Cellulose (Cl^-) column (1.5 × 14 cm). Initially, elution was performed using 40 mL of distilled water at a flow rate of 1.0 mL/min, followed by a linear gradient from 0.0 to 0.5 M NaCl (160 mL) using a gradient mixer to analyze the homogeneity of its charge distribution. [18]. The elution curve was obtained by determining the distribution of total sugar and uronic acid content. And then, WHNP-A (10 g) was loaded onto a DEAE-Cellulose column and eluted stepwise with distilled water, 0.2 M, 0.3 M, and 0.5 M NaCl solution, resulting in four fractions named WHNP-AH, WHNP-A2, WHNP-A3, and WHNP-A5 [20]. Two major fractions (WHNP-A2 and WHNP-A3) were then eluted with 0.15 M NaCl at a flow rate of 0.15 mL/min using a Sepharose CL-6B column (1.5 × 90 cm), respectively. Fractions (3 mL per tube) were collected based on the total sugar and uronic acid content. Selected fractions were combined, dialyzed and freeze-dried, finally obtaining three major pectin fractions WHNP-A2b, WHNP-A2c and WHNP-A3b, respectively.

UV spectroscopy

A polysaccharide sample (2 mg) was dissolved in 4 mL of distilled water. UV–vis absorption spectra were recorded in the scan range from 190 to 800 nm using a Shimadzu UV-2700 spectrophotometer.

FT-IR spectroscopy

A polysaccharide sample was ground with KBr powder and pressed into a 1 mm pellet. FT-IR spectra (4000 to 500 cm^{-1}) were obtained using a PerkinElmer Spectrum Two FT-IR spectrometer (Perkin Elmer, USA).

Methylation analysis

The reduction of uronic acid was performed following the method described by Pettolino, Walsh, Fincher and Bacic [21]. Carboxyl groups in uronic acids were activated using carbodiimide regents and then reduced to their neutral sugars by $NaBD_4$. The reduced pectic polysaccharides (5 mg) were dissolved in dimethylsulfoxide

(DMSO, 0.5 mL) and stirred at room temperature for 30 min. Methylation was carried out by adding NaOH-DMSO (0.5 mL) and subsequently iodomethane (1 mL) [22]. The methylation reaction was stopped by adding water (2 mL). The methylated products were extracted with chloroform (2 mL) and dried under a nitrogen stream. After hydrolysis with 2 M TFA at 120 °C for 3 h, reduction with $NaBH_4$ and acetylation with acetic anhydride and pyridine, the partially methylated alditol acetates (PMAA) were analyzed using gas chromatography-mass spectrometry (GC–MS; 7890B-5977B, Agilent, USA) on a DB-35 ms capillary column (30 m × 0.32 mm × 0.25 mm). PMAAs were identified using their typical electron impact decomposition profiles and retention times, and compared to partially methylated standards from the Complex Carbohydrate Research Center Database (http://www.ccrc.uga.edu/specdb/ms/pmaa/pframe.html).

NMR spectroscopy

Polysaccharide samples were dissolved in D_2O (0.5 mL, 99.8%) and stirred overnight at room temperature. ^{13}C-NMR spectra were recorded at 20 °C using a Bruker Avance 600 MHz NMR spectrometer (Bruker Inc., Rheinstetten, Germany). Acetone was used as the internal standard.

Enzymatic hydrolysis

WHNP-A2c (5 mg/mL each) was dissolved in 50 mM HAc-NaAc solution (sodium acetate buffer, pH 4.5). The fraction was then incubated with endo-polygalacturonase (0.04 U per mg of sample) at 40 °C for 12 h, repeated once. The enzyme was denatured by boiling at 100 °C for 10 min, after which the hydrolysate was centrifuged at 4500 rpm for 20 min. The supernatant was loaded onto a Sephadex G-75 column (3.0 × 90 cm), and eluted with 0.15 M NaCl at a flow rate of 0.4 mL/min. Eluates (8 mL per tube) were collected and assayed by the total carbohydrate content. The appropriate fractions were combined. Polysaccharide fractions were desalted using dialysis tubes with 1 kDa cutoff and oligosaccharide fractions were desalted using Sephadex G-10 column, finally obtaining three sub-fractions (A2c-E1, A2c-E2 and A2c-E3), respectively.

ESI–MS analysis of oligosaccharides from enzymatic hydrolysis

ESI–MS detection was performed in the negative mode with a capillary voltage of 4000 V, a capillary temperature of 200 °C and dry gas flow rate of 2 L/min. Mass spectra were recorded in the range of m/z 100 ~ 3000. The acquired data were processed using the Trap-control software.

Results

Purification of water-soluble polysaccharides

Water-soluble polysaccharides were obtained from the dried leaves of *Hedera nepalensis* using hot water extraction and ethanol-based precipitation methods. The yield of WHNP (for water-soluble *Hedera nepalensis* polysaccharides) was 4.0%. Monosaccharide composition analysis revealed that WHNP was mainly composed of galacturonic acid (GalA, 26.4%), galactose (Gal, 20.2%), glucose (Glc, 19.0%), arabinose (Ara, 14.6%), rhamnose (Rha, 8.6%), trace amounts of Man (4.8%), GlcA (3.5%) and Xyl (1.7%) (Table 1).

WHNP was purified and fractionated using anion-exchange and size-exclusion chromatographies (Fig. 1). The purification scheme for polysaccharides from the leaves of *Hedera nepalensis* was illustrated in Fig. 1. WHNP was first separated into two fractions using anion-exchange chromatography (Fig. 2A). As a result, two purified fractions, neutral polysaccharide fraction WHNP-N (yield of 72.0%) and acidic polysaccharide fraction WHNP-A (yield of 15.1%) was obtained from WHNP. WHNP-N was mainly composed of Glc (47.9%), with some Gal (22.0%), Ara (11.6%), Man (4.5%) and Xyl (1.9%) (Table 1). In this paper, for the neutral polysaccharide fraction WHNP-N, further analysis was not conducted anymore. The major monosaccharide composition in WHNP-A was GalA (32.8%), Rha (13.5%), Gal (19.5%) and Ara (10.1%) (Table 1), which indicated that acidic polysaccharide fraction mainly contained the pectic polysaccharide.

WHNP-A was further applied to an analytical DEAE-Cellulose column (Fig. 2B), which pointed out that WHNP-A has an inhomogeneous charge distribution. Thus, WHNP-A was further separated by utilizing a preparative DEAE-Cellulose column, and four fractions WHNP-AH (yield 0.2%), WHNP-A2 (yield 3.3%), WHNP-A3 (yield 1.6%) and WHNP-A5 (yield 1.1%) fractions were obtained, respectively (Table 1). Due to the low yield, WHNP-AH and WHNP-A5 fractions were not further investigated. The major fractions (WHNP-A2 and WHNP-A3) were loaded onto a Sepharose CL-6B column to obtain three fractions WHNP-A2a (yield 0.2%), WHNP-A2b (yield 1.1%) and WHNP-A2c (yield 0.6%) from WHNP-A2, and two fractions WHNP-A3a (yield 0.1%) and WHNP-A3b (yield 0.9%) from WHNP-A3, respectively (Fig. 2C and D). Therefore, WHNP-A2b, WHNP-A2c and WHNP-A3b were the major polysaccharide fractions separated from WHNP-A2 and WHNP-A3, respectively. In UV spectra (Additional file 1: Figure S1), no UV absorption was observed at 260 nm and 280 nm, indicating the absence of proteins and nucleic acids in all purified polysaccharides.

Table 1 Yields and monosaccharide compositions of polysaccharides from *Hedera nepalensis*

Fractions	Yield (w %)	TBA assay	Monosaccharide composition (mol%)							
			GalA	Rha	Gal	Ara	Glc	GlcA	Xyl	Man
WHNP	4.0	ND[b]	26.4	8.6	20.2	14.6	19.0	3.5	1.7	4.8
WHNP-N	72.0[a]	ND[b]	–	–	22.0	11.6	47.9	–	1.9	4.5
WHNP-A	15.1[a]	ND[b]	32.8	13.5	19.5	10.1	7.5	5.7	2.4	6.8
WHNP-AH	0.2[a]	ND[b]	–	–	44.9	4.6	19.4	–	2.1	25.9
WHNP-A2	3.3[a]	ND[b]	28.4	14.7	24.1	11.4	4.7	3.0	2.2	5.7
WHNP-A3	1.6[a]	ND[b]	27.2	20.9	17.1	8.2	10.2	4.8	2.0	5.5
WHNP-A5	1.1[a]	ND[b]	7.5	6.0	20.1	5.9	22.6	13.0	2.0	12.3
WHNP-A2a	0.2[a]	ND[b]	5.6	9.6	25.1	4.5	20.1	3.7	5.9	15.8
WHNP-A2b	1.1[a]	–[d]	20.9	18.9	33.5	21.7	1.2	1.6	–	1.9
WHNP-A2c	0.6[a]	+[c]	60.8	8.4	12.6	14.5	0.8	1.1	–	1.5
WHNP-A3a	0.1[a]	ND[b]	6.3	7.0	23.7	4.2	23.0	9.0	2.9	17.3
WHNP-A3b	0.9[a]	–[d]	30.8	29.1	18.7	14.5	1.9	2.5	1.0	1.3

[a] Yield in relation to WHNP

[b] ND: Not determined

[c] "+" Positive result indicating the presence of RG-II domain

[d] "-" Negative result

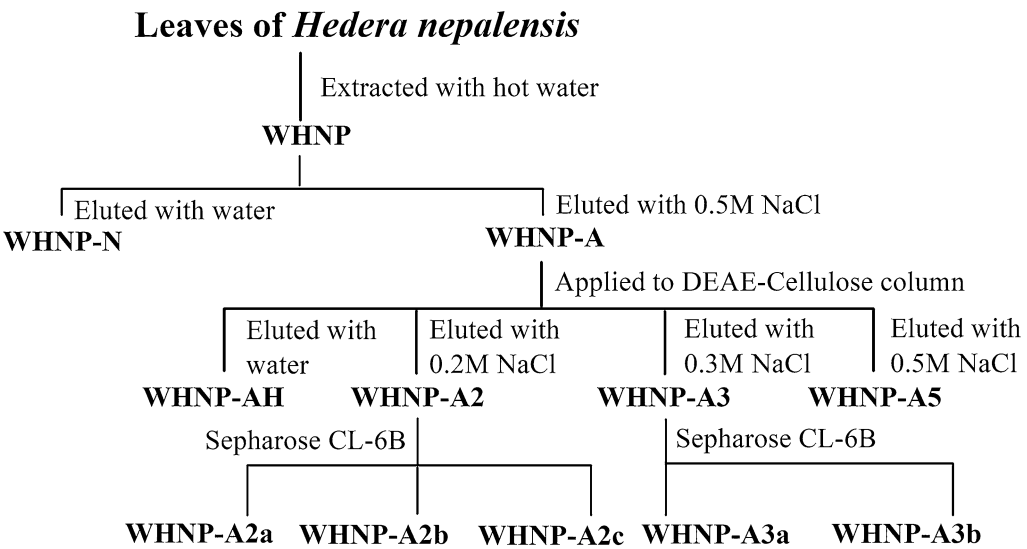

Fig. 1 Purification scheme for polysaccharides from *Hedera nepalensis*

Sugar composition and molecular weight distribution

The major monosaccharide constituents in WHNP-A2a and WHNP-A3a were GalA (5.6%, 6.3%), Rha (9.6%, 7.0%), Gal (25.1%, 23.7%), Ara (4.5%, 4.2%) and Glc (20.1%, 23.0%), respectively (Table 1). The primary monosaccharide composition in WHNP-A2b and WHNP-A3b were GalA (20.9%, 30.8%), Rha (18.9%, 29.1%), Gal (33.5%, 18.7%) and Ara (21.7%, 14.5%) (Table 1). In these two fractions, the ratio of Rha/GalA was 0.9 and 0.94, respectively, typical for RG-I-type pectins. Also, WHNP-A2c contained GalA (60.8%) as the major monosaccharide, followed by Rha (8.4%), Ara (14.5%) and Gal (12.6%). TBA assay is a very sensitive reaction used to identify Kdo and Dha, which are characteristic monosaccharides in RG-II [19, 23]. WHNP-A2c fraction contained a TBA-positive constituent, indicating the presence of the RG-II domain in this fraction (Table 1).

For these purified polysaccharide fractions, the homogeneity and molecular weight were determined by HPSEC (Fig. 3). WHNP-A2a and WHNP-A3a had higher

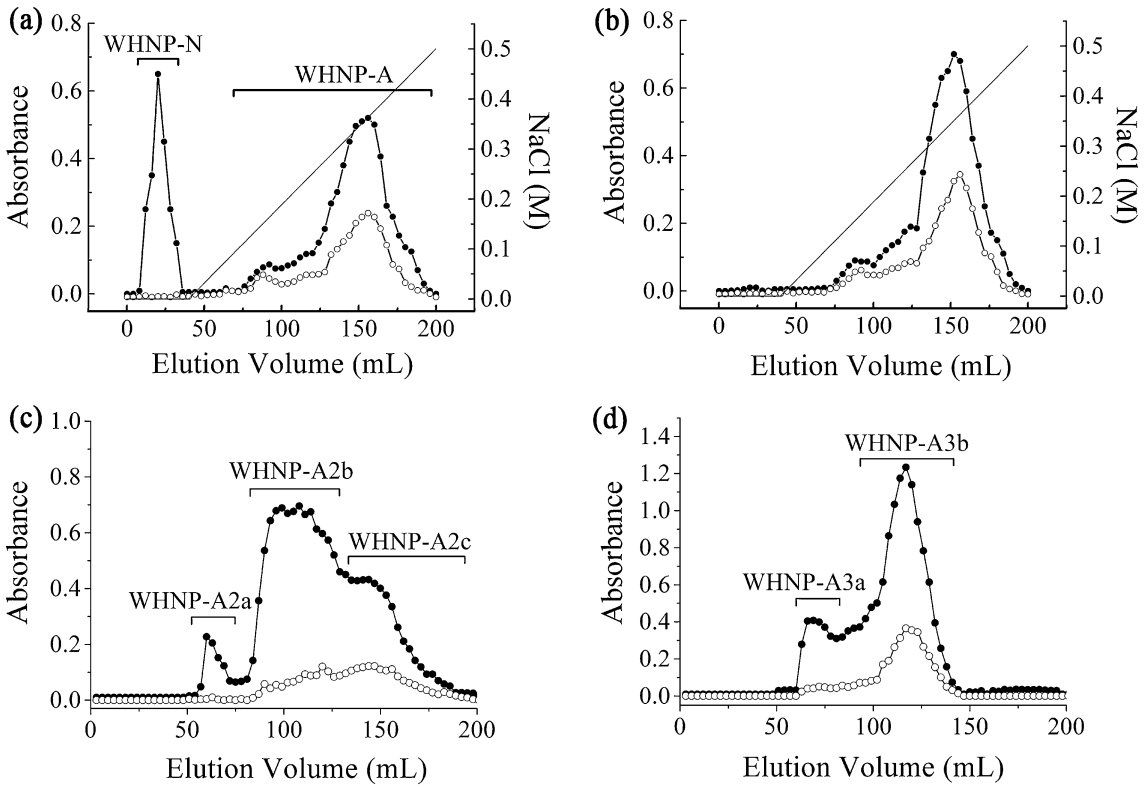

Fig. 2 Elution profiles of **a** WHNP and **b** WHNP-A on DEAE-Cellulose column, eluted by a linear gradient of NaCl, respectively. Elution profiles of **c** WHNP-A2 and **d** WHNP-A3 on Sepharose CL-6B column. (-●-, total sugar; -○-, uronic acid)

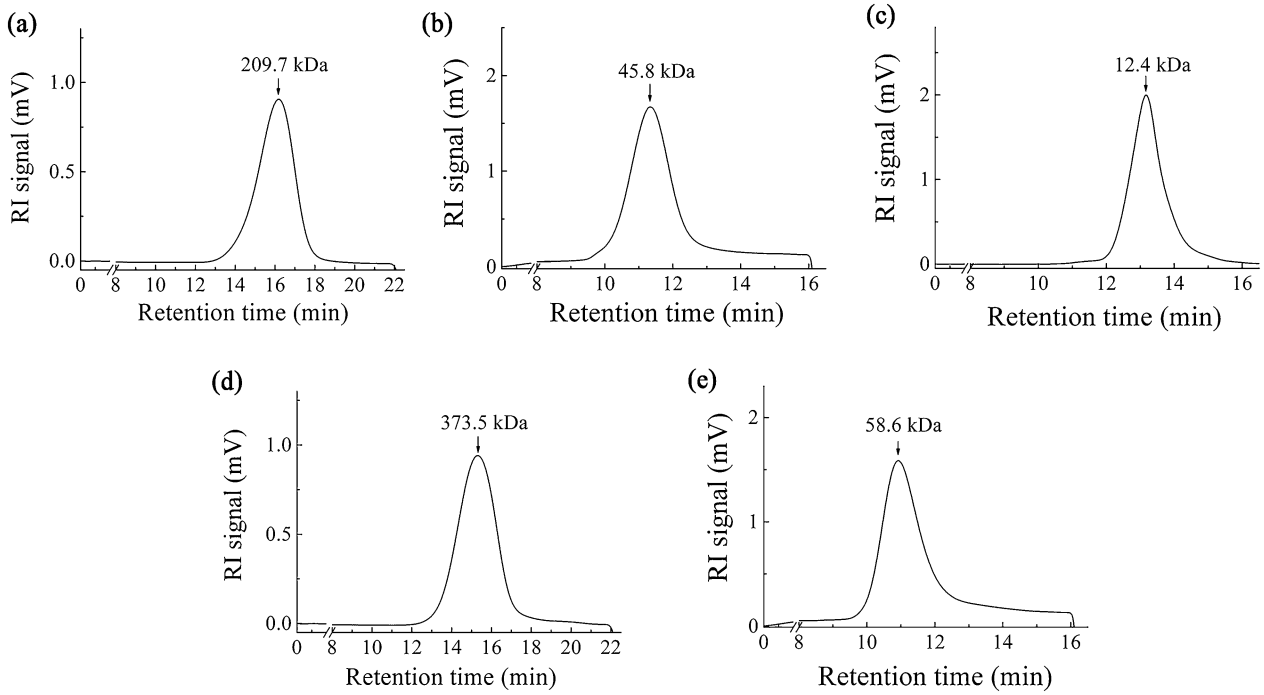

Fig. 3 HPSEC elution profiles of purified polysaccharide fractions. **a** WHNP-A2a and **d** WHNP-A3a on TSK-gel G-4000 PWXL column. **b** WHNP-A2b, **c** WHNP-A2c and **e** WHNP-A3b on TSK-gel G-3000 PWXL column

molecular weights of 209.7 kDa and 373.5 kDa, while WHNP-A2b, WHNP-A2c and WHNP-A3b had lower molecular weights of 45.8 kDa, 12.4 kDa and 58.6 kDa, respectively. As can be seen in Fig. 3, all fractions showed homogeneous distributions. In this paper, the structures of WHNP-A2b, WHNP-A2c and WHNP-A3b were studied in more detail.

FT-IR analysis of WHN-A2b, WHNP-A2c and WHNP-A3b

The results of FT-IR spectrum analyses for WHNP-A2b, WHNP-A2c and WHNP-A3b are presented in Fig. 4. As shown in Fig. 4, the strong and wide peak near 3400 cm^{-1} was attributed to the stretching vibration of the hydroxyl group (-OH), which was associated with intermolecular and intramolecular hydrogen bonding. Weak peaks observed around 2935 cm^{-1} indicated the absorption of C-H bonds, involving the stretching and bending vibrations of CH, CH_2, and CH_3 [24]. Peaks around 1740 cm^{-1} and 1617 cm^{-1} were assigned to the stretching vibrations of the C=O bonds in methyl-esterified and ionic carboxyl groups, respectively [25]. The degree of methyl-esterification (DM) could be determined by analyzing these two peak intensities [26]. As a result, the observed DM values for WHNP-A2b, WHNP-A2c and WHNP-A3b were 15.5%, 24.4%, and 6.1%, respectively. These results indicated that the DM of WHNP-A2c was higher than that of WHNP-A2b and WHNP-A3b. Besides, the band near 1400 cm^{-1} was assigned to C-H deformation and vibrations. It could be seen that peaks observed in the region between 1010 cm^{-1} and 1100 cm^{-1} were attributed to the absorption of skeletal C–C and C-O vibrations of glycosidic bonds and pyranoid rings [27]. The characteristic peaks around 890 cm^{-1} and 830 cm^{-1} indicated the presence of β-linked and α-linked sugar residues, respectively [28].

Methylation analysis of WHNP-A2b, WHNP-A2c and WHNP-A3b

The glycosidic linkages in WHNP-A2b, WHNP-A2c and WHNP-A3b were determined through methylation analysis, and the results were listed in Table 2. The GC–MS results were presented in Additional file 1: Figure S2. As observed, 1,4-linked Gal*p*A was the major linkage type in WHNP-A2b (19.6%), WHNP-A2c (61.3%) and WHNP-A3b (32.7%). Rha residues were in the form of 1,2-linked Rha and 1,2,4-linked Rha. These results indicated that these fractions might contain both HG and RG-I domains. The Rha units in the backbone of RG-I were branched at O-4, and the degrees of branching were estimated to be 45.2%, 33.8% and 33.7% for WHNP-A2b, WHNP-A2c and WHNP-A3b, respectively. Ara residues existed in the form of terminated-linked, 1,3-linked, 1,5-linked and 1,3,5-linked in WHNP-A2b and WHNP-A3b, while in WHNP-A2c, Ara residues were present as terminated-linked, 1,5-linked and 1,3,5-linked Ara. Gal residues were mainly present in the form of terminal-linked, 1,3-linked, 1,6-linked and 1,3,6-linked in WHNP-A2b, WHNP-A2c and WHNP-A3b. These glycosidic linkages suggested the presence of arabinan

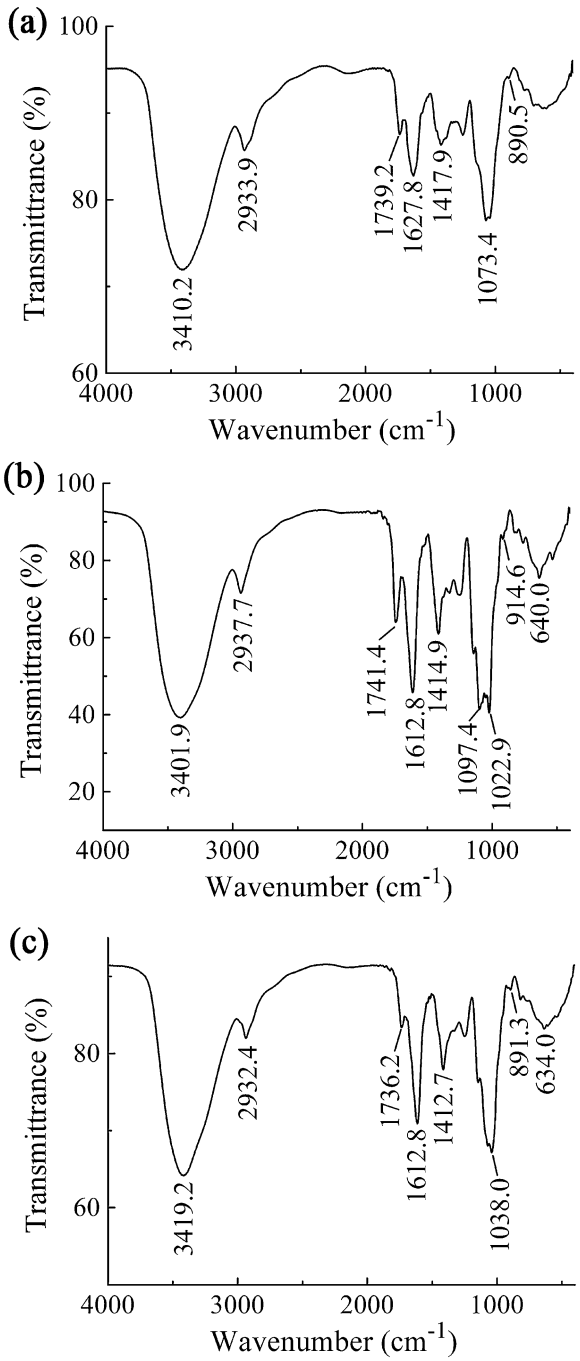

Fig. 4 The FT-IR spectra of **a** WHNP-A2b, **b** WHNP-A2c and **c** WHNP-A3b

Table 2 The glycosidic linkage type and molar percentage of WHNP-A2b, WHNP-A2c, WHNP-A3b and A2c-E1 based on methylation and GC–MS

Sugar Residues	Molar percentage (%)			
	WHNP-A2b	WHNP-A2c	WHNP-A3b	A2c-E1
1,4-Gal*p*A	19.6	61.3	32.7	21.1
1,2–Rha*p*	8.0	4.9	20.1	9.6
1,2,4-Rha*p*	6.6	2.5	10.2	7.2
Terminal-Gal*p*	7.0	2.2	9.1	7.8
1,3-Gal*p*	7.2	0.7	2.2	4.3
1,6-Gal*p*	4.0	1.9	1.8	1.9
1,3,6-Gal*p*	13.9	5.0	3.5	9.1
1,4-Gal*p*	2.4	3.9	3.4	4.1
1,4,6-Gal*p*	1.0	–	–	0.6
1,3,4-Gal*p*	0.9	–	–	1.1
Terminal-Ara*f*	13.2	6.0	3.9	8.2
1,3-Ara*f*	1.4	–	1.1	1.5
1,5-Ara*f*	8.3	7.1	6.4	9.5
1,3,5-Ara*f*	2.2	2.1	0.8	5.1

or AG-II side chains in these fractions [21]. Additionally, small amounts of 1,4-linked-Gal*p* were detected in WHNP-A2b, WHNP-A2c and WHNP-A3b, and 1,3,4/1,4,6-linked-Gal*p* were also detected in WHNP-A2b, indicating the possible existence of minor 1,4-linked galactan or AG-I side chains in these fractions [22].

^{13}C NMR spectra analysis of WHNP-A2b, WHNP-A2c and WHNP-A3b

The chemical structures of WHNP-A2b, WHNP-A2c, and WHNP-A3b were further analyzed using ^{13}C NMR spectra (Fig. 5), and the chemical shift assignments are presented in Table 3.

The anomeric carbons of non-esterified α-D-1,4-Gal*p*A at 96.43 ppm, 98.41 ppm and 96.40 ppm were also detected in WHNP-A2b, WHNP-A2c and WHNP-A3b, respectively [29]. The signals around 174.03 ppm were assigned to C-6 of non-esterified α-D-1,4-Gal*p*A residues, respectively [29]. The signals around 51.82 ppm and 19.56 ppm were attributed to methyl and acetyl groups attached to α-D-Gal*p*A units, respectively, further confirming the esterification of HG [30]. These resonance signals showed that three major fractions contained HG-type pectins. The anomeric carbon of methyl-esterified α-D-1,4-Gal*p*A at 99.35 ppm was also detected in WHNP-A2c [30]. The intensity signals for methyl-esterified residues in the ^{13}C NMR spectra of these fractions were consistent with their FT-IR spectra, respectively. In WHNP-A2b, WHNP-A2c and WHNP-A3b, the anomeric signals at 97.48 ppm, 97.97 ppm and 97.72 ppm were assigned to C-1 groups of α-L-1,2-Rha*p*/α-L-1,2,4-Rha*p*, respectively [30, 31]. Also, C-6 groups of α-L-1,2-Rha*p* and α-L-1,2,4-Rha*p* gave signals around 15.51 ppm and 15.73 ppm in the high-field region, respectively [30, 31], indicating that RG-I-type pectins were contained in these fractions. In WHNP-A2b, the signals at 103.88 ppm, 101.56 ppm, 102.43 ppm and 103.29 ppm were assigned to the anomeric carbon of β-D-1,4-Gal*p*, β-D-1,3,6-Gal*p*, β-D-1,3/1,6-Gal*p* and β-terminal-Gal*p*, while in WHNP-A2c, the signals at 101.88 ppm, 102.42 ppm and 102.88 ppm were attributed to C-1 of β-D-1,3,6-Gal*p*, β-D-1,3/1,6-Gal*p* and β-terminal-Gal*p*, respectively (Table 3) [31–36]. In WHNP-A3b, the signals at 102.18 ppm, 102.38 ppm and 103.53 ppm were assigned to the anomeric carbon of β-D-1,3,6-Gal*p*, β-D-1,3/1,6-Gal*p* and β-terminal-Gal*p*, respectively [31–36]. Besides, in WHNP-A2b, the resonances at 108.20 ppm, 106.42 ppm and 106.05 ppm originated from the anomeric carbons of α-terminal-Ara*f*, α-L-1,5-Ara*f* and α-L-1,3,5-Ara*f*, while in WHNP-A2c, the anomeric carbon resonances of α-terminal-Ara*f*, α-1,5-Ara*f* and α-1,3,5-Ara*f* were clearly identified at 108.30 ppm, 106.42 ppm and 105.98 ppm, respectively [31–33]. In WHNP-A3b, the signal at 108.27 ppm, 106.42 ppm and 106.15 ppm were assigned to anomeric carbon resonances of α-terminal-Ara*f*, α-1,5-Ara*f* and α-1,3,5-Ara*f*, respectively. Also, signals at 95.08 ppm and 91.12 ppm were assigned to C-2 of α-Kdo*p* and α-Ace*f*A, indicating RG-II domain existed in WHNP-A2c [23, 37]. In WHNP-A2b and WHNP-A3b, the characteristic signals for RG-II domain were not found, suggesting NMR results were consistent with TBA assay results in these fractions. Also, the complex, overlapping signals at 60 ppm-85 ppm are attributed to C-2 to C-5 groups of different linkages in α-L-Ara*f* and α-L-Rha*p*, and C-2 to C-6 groups of β-D-Gal*p* and α-D-Gal*p*A [38, 39]. These assignments are summarized in Table 3. Further analyses of the NMR spectra indicated that both WHNP-A2b and WHNP-A3b contained HG and RG-I domains, while WHNP-A2c was composed of HG, RG-II and RG-I domains. Also, the results showed that in WHNP-A2b, the RG-I domains might contain α-L-1,5/1,3,5-arabinan, β-D-1,4-galactan and AG-II as side chains, while in WHNP-A2c and WHNP-A3b, α-L-1,5/1,3,5-arabinan and AG-II as side chains are contained as side chains in RG-I domains.

Enzymatic analysis of WHNP-A2c

In order to further study the structural features of WHNP-A2c, it was hydrolyzed using endo-polygalacturonase (Endo-PG), which specifically degrades un-esterified α-D-1,4-galacturonans in HG-type pectins [33]. After the enzymatic hydrolysis, the degradation products of WHNP-A2c were separated into three sub-fractions

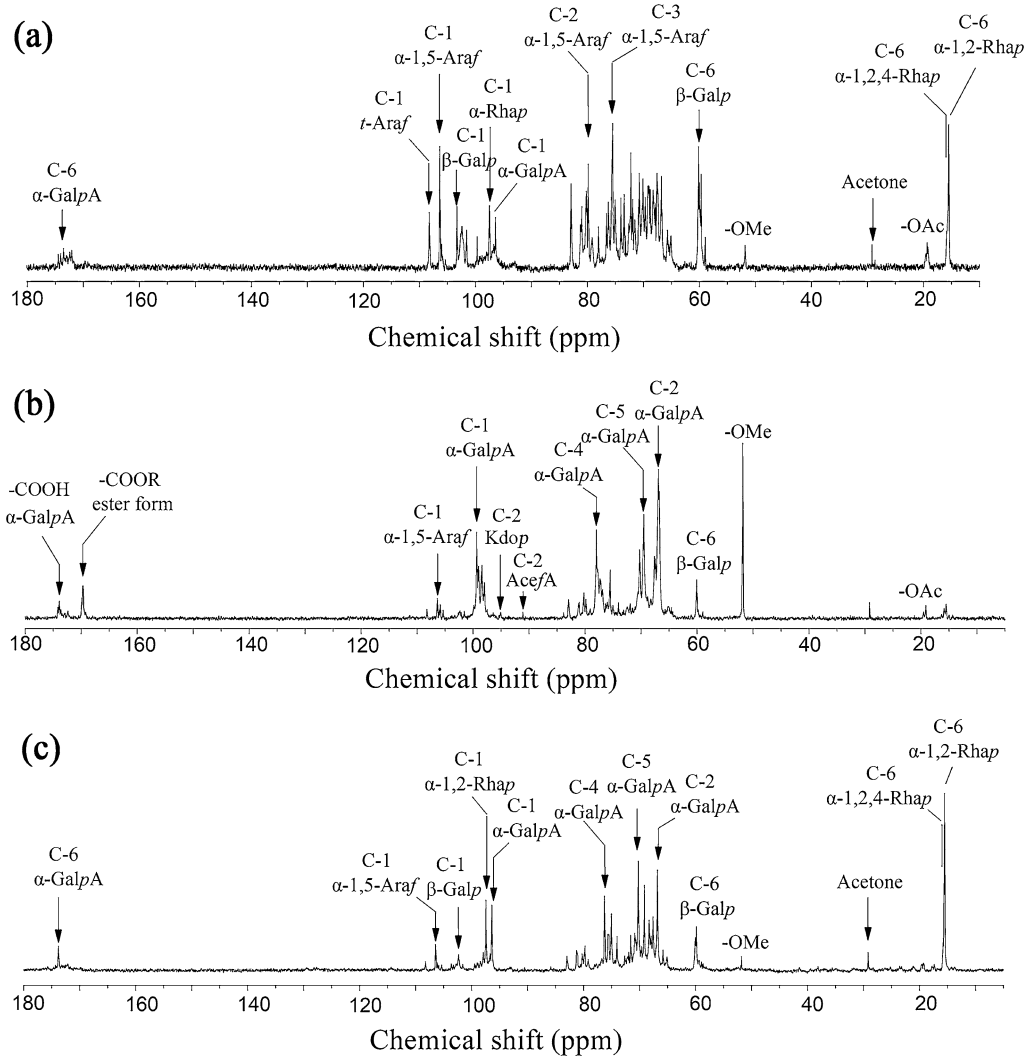

Fig. 5 The ^{13}C NMR spectra of (**a**) WHNP-A2b, (**b**) WHNP-A2c and (**c**) WHNP-A3b

(A2c-E1, A2c-E2, and A2c-E3) using size-exclusion chromatography, as depicted in Fig. 6A. Their molecular weight distributions were represented in Fig. 6B.

In A2c-E1, the monosaccharide compositions mainly consisted of GalA (22.7%), Rha (19.9%), Gal (24.4%) and Ara (21.5%) (Table 4), while the ratio of Rha/GalA was 0.9, suggesting this fraction mainly contained RG-I-type domains. Comparing the monosaccharide compositions of WHNP-A2c, after the enzymatic hydrolysis, the amounts of GalA in A2c-E1 relatively decreased, whereas the amounts of Gal and Ara correspondingly increased (Table 4). In A2c-E1, the sum for the amounts of Gal and Ara was 45.9%, while the ratio of (Gal + Ara)/Rha was 2.3, indicating the presence of short neutral sugar side chains in this fraction [34]. The positive result from the TBA assay indicated that A2c-E2 primarily consisted of RG-II-type domains. As can be shown in Table 4, monosaccharide compositions and molecular weight distributions of A2c-E2 were also in agreement with RG-II type structural features [23, 40]. A2c-E3 (molecular weights < 2 kDa) mainly consisted of GalA (90.1%), indicating that it was oligosaccharides produced by the degradation of HG domains.

Based on these analysis results, it can be concluded that WHNP-A2c is composed of RG-I, RG-II and HG domains with mass ratios of 1.8:1.0:0.6. Therefore, it can be considered that RG-I is the predominant domain in WHNP-A2c. Due to the well-studied structure of RG-II domains, A2c-E2 (RG-II domains) was not further analyzed in this study. We focused on analyzing the chemical structure of RG-I domain (A2c-E1) and HG fraction (A2c-E3) isolated from WHNP-A2c.

Table 3 Chemical shifts of the ^{13}C-NMR spectra of WHNP-A2b, WHNP-A2c and WHNP-A3b

Fractions	Sugar Residues	Chemical Shifts, δ (ppm)					
		C-1	C-2	C-3	C-4	C-5	C-6
WHNP-A2b	→4)-α-Gal*p*A-(1→	96.43	67.59	68.28	76.27	70.10	174.03
	→2)-α-Rha*p*-(1→	97.48	75.49	69.20	71.89	70.75	15.51
	→2,4)-α-Rha*p*-(1→	97.48	75.49	69.20	74.09	70.75	15.73
	→4)-β-Gal*p*-(1→	103.88	71.68	73.22	77.39	74.49	59.69
	t-β-Gal*p*-(1→	103.29	71.61	72.26	76.10	73.55	60.18
	→3)-β-Gal*p*-(1→	102.43	71.61	79.89	68.27	74.89	59.89
	→6)-β-Gal*p*-(1→	102.43	70.88	72.26	68.27	74.89	67.59
	→3,6)-β-Gal*p*-(1→	101.56	71.61	79.89	68.27	74.89	67.59
	→5)-α-Ara*f*-(1→	106.42	81.00	75.48	82.85	65.70	–
	→3,5)-α-Ara*f*-(1→	106.05	79.94	81.26	82.85	65.70	–
	t-α-Ara*f*-(1→	108.20	81.00	75.68	82.85	60.07	–
WHNP-A2c	→4)-α-Gal*p*A-(1→	98.41	66.90	67.30	76.90	70.10	173.75
	→4)-α-Gal*p*A(OMe)-(1→	99.35	–	67.60	77.90	70.10	169.86
	→2)-α-Rha*p*-(1→	97.97	75.50	69.52	–	70.27	15.52
	→2,4)-α-Rha*p*-(1→	97.97	75.50	69.52	74.02	70.27	15.88
	t-β-Gal*p*-(1→	102.88	71.40	72.58	75.67	74.92	60.10
	→3)-β-Gal*p*-(1→	102.42	71.40	79.88	67.35	74.92	58.98
	→6)-β-Gal*p*-(1→	102.42	71.40	72.58	67.35	74.92	67.10
	→3,6)-β-Gal*p*-(1→	101.88	71.40	79.88	67.35	74.92	67.10
	→5)-α-Ara*f*-(1→	106.42	81.09	75.48	82.95	65.70	–
	→3,5)-α-Ara*f*-(1→	105.98	80.01	82.69	82.95	65.70	–
	t-α-Ara*f*-(1→	108.30	81.09	–	82.95	60.08	–
WHNP-A3b	→4)-α-Gal*p*A-(1→	96.40	66.79	69.20	76.40	70.20	172.67
	→2)-α-Rha*p*-(1→	97.72	75.10	68.31	71.86	69.22	15.39
	→2,4)-α-Rha*p*-(1→	97.72	75.10	68.31	74.00	–	15.67
	t-β-Gal*p*-(1→	103.53	71.60	72.36	75.06	74.08	60.03
	→3)-β-Gal*p*-(1→	102.38	71.60	79.20	67.67	74.08	58.89
	→6)-β-Gal*p*-(1→	102.38	71.60	72.36	67.67	74.08	67.08
	→3,6)-β-Gal*p*-(1→	102.18	71.60	79.20	67.67	74.08	67.08
	→5)-α-Ara*f*-(1→	106.42	81.18	75.50	83.01	65.65	–
	→3,5)-α-Ara*f*-(1→	106.15	79.89	82.71	83.01	65.65	–
	t-α-Ara*f*-(1→	108.27	81.18	75.66	83.01	60.06	–

Structural analysis of RG-I and HG domains from WHNP-A2c

The glycosidic linkages in RG-I domain (A2c-E1) were determined using methylation analysis and listed in Table 2. GC–MS result was shown in Additional file 1: Fig. S2. The result showed that GalA residues were present as 1,4-linked Gal*p*A, and Rha residues in the form of 1,2-linked and 1,2,4-linked Rha*p*. The molar percentages of glycosidic linkages for GalA and Rha in A2c-E1 were nearly identical, which was typical for RG-I domain. The Rha residues within the RG-I backbone exhibited branching at O-4, with an estimated branching degree of 42.9% for A2c-E1. Ara residues were found in the form of terminal-linked, 1,3-linked, 1,5-linked, and 1,3,5-linked structures within A2c-E1, with 1,5-linked Ara residues being the most dominant. Gal residues were observed in the form of terminal-linked, 1,3-linked, 1,6-linked and 1,3,6-linked structures in A2c-E1. These glycosidic linkages indicated that A2c-E1 might contain arabinan or AG-II side chains [21]. Meanwhile, small amounts of 1,4-linked-Gal*p* (4.1%), 1,4,6-linked-Gal*p* (0.6%) and 1,3,4-linked-Gal*p* (1.1%) were detected in A2c-E1, indicating the possible presence of minor galactan and/or AG-I as side chains [22].

To further study the chemical structure of the RG-I domain (A2c-E1) isolated from WHNP-A2c, it was analyzed using ^{13}C NMR spectroscopy. In the ^{13}C NMR spectrum of A2c-E1 (Fig. 7A), signals at 96.40, 67.10, 68.20,

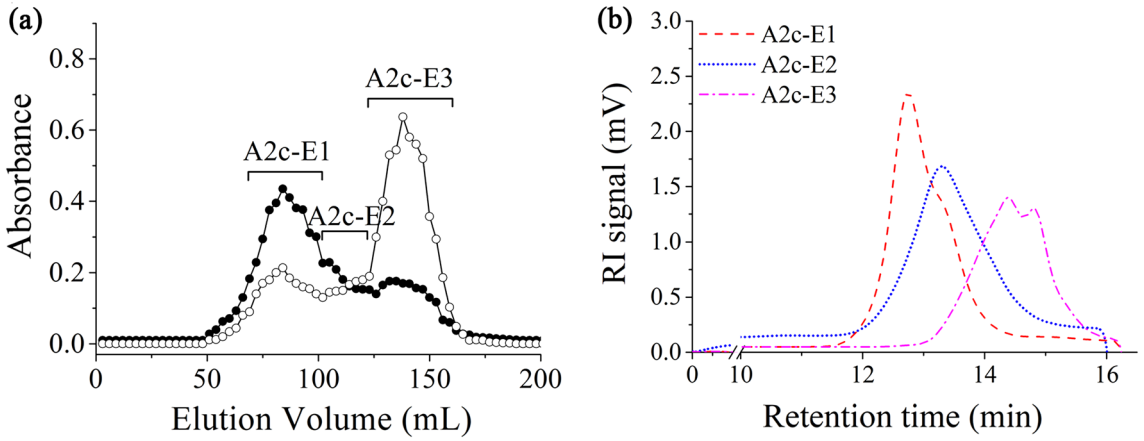

Fig. 6 **(a)** Elution profiles of WHNP-A2c hydrolysates on Sephadex G-75 column (-●-, total sugar; -○-, uronic acid). **(b)** HPSEC elution profiles of three sub-fractions of WHNP-A2c on TSK-gel G-3000 PWXL column

Table 4 Yields, Mws, TBA assay, and sugar compositions of sub-fractions obtained by Endo-PG hydrolysis from WHNP-A2c

Fractions	Yield (w %)	Mw (kDa)	TBA assay	Monosaccharide composition (mol%)							
				GalA	Rha	Gal	Ara	Glc	GlcA	Xyl	Man
A2c-E1	45.0[a]	15.5	–	22.7	19.9	24.4	21.5	2.4	2.5	3.4	2.6
A2c-E2	25.5[a]	8.5	+	62.4	16.2	8.7	10.1	0.8	1.2	–	0.5
A2c-E3	16.2[a]	2.3	–	90.1	2.8	1.5	1.6	2.5	–	–	1.2

[a] Yield in relation to WHNP-A2c; "-" Negative result; " + " Positive result

76.20, 70.11 and 173.57 ppm can be assigned to C-1 to C-6 of α-1,4-GalA, respectively (Table 5) [29, 30] 25,26. The signal at 97.48 ppm was attributed to C-1 of α-L-1,2-Rha*p*/α-L-1,2,4-Rha*p*, and signals at 15.52 ppm and 15.75 ppm were assigned to C-6 of these two residues, respectively [29, 30]. These results confirmed that A2c-E1 was composed of a RG-I backbone. The anomeric carbon resonances of α-terminal-Ara*f*, α-1,5-Ara*f* and α-1,3,5-Ara*f* were clearly identified at 108.20 ppm, 106.35 ppm, and 106.01 ppm, respectively [31]. Three major peaks at 103.96 ppm, 103.29 ppm, 102.38 ppm and 101.59 ppm appeared in the spectrum of A2c-E1, representing C-1 of 1,4-, terminal-, 1,3/1,6- and 1,3,6-linked-β-D-Gal*p*, respectively [31–36, 41]. Based on these results, it could be seen that A2c-E1 was a RG-I-type pectin branched with α-L-1,5/1,3,5-arabinan, β-D-1,4-galactan and/or AG-I and AG-II as side chains, which was consistent with methylation analysis.

A2c-E3 was oligogalacturonic acids obtained from the degradation of non- or low-methyl-esterified HG domains of WHNP-A2c. The structural features of A2c-E3 were analyzed in more detail using ESI–MS [39, 42–44]. As shown in Fig. 7B, the oligosaccharide fragments in A2c-E3 included non-esterified monomer 1^{00}-type ion (m/z 193), dimer 2^{00}-type ion (m/z 369) and trimer 3^{00}-type ion (m/z 545). GalA dimer 2^{10}-type ion (m/z 383), trimer 3^{10}-type ion (m/z 559), tetramers 4^{10}-H_2O-type ion (m/z 717), 4^{10}-type ion (m/z 735) and 4^{20}-type ion (m/z 749) that contained one to two methyl-esters were identified. Also, GalA oligomers with DP 5–7 carrying two to three methyl-esters groups 5^{30}-type ion (m/z 925), 6^{20}-type ion (m/z 1101) and 6^{30}-type ion (m/z 1115) were detected. Besides, more oligogalacturonic acids containing methyl-esters groups and one acetyl group were detected in A2c-E3; e.g. GalA oligomers with DP 4–7 carrying one to three methyl-esters groups and one acetyl group 4^{11}-type ion (m/z 777), 6^{31}-type ion (m/z 1157) and 7^{31}-type ion (m/z 1333). To sum up, it can be deduced that WHNP-A2c contains HG domains with a high degree of methyl esterification, which aligns with the FT-IR and NMR results.

Discussion

According to previous studies, the chemical compounds isolated from the dried leaves of *Hedera nepalensis* have been reported to exhibit diverse bioactivities, such as antifungal, antimicrobial, antioxidant and antitumor capacities [1–11]. These studies primarily focused on the structural features of phytochemicals, such as alkaloids, glycosides, flavonoids, steroids, tannins and terpenoids.

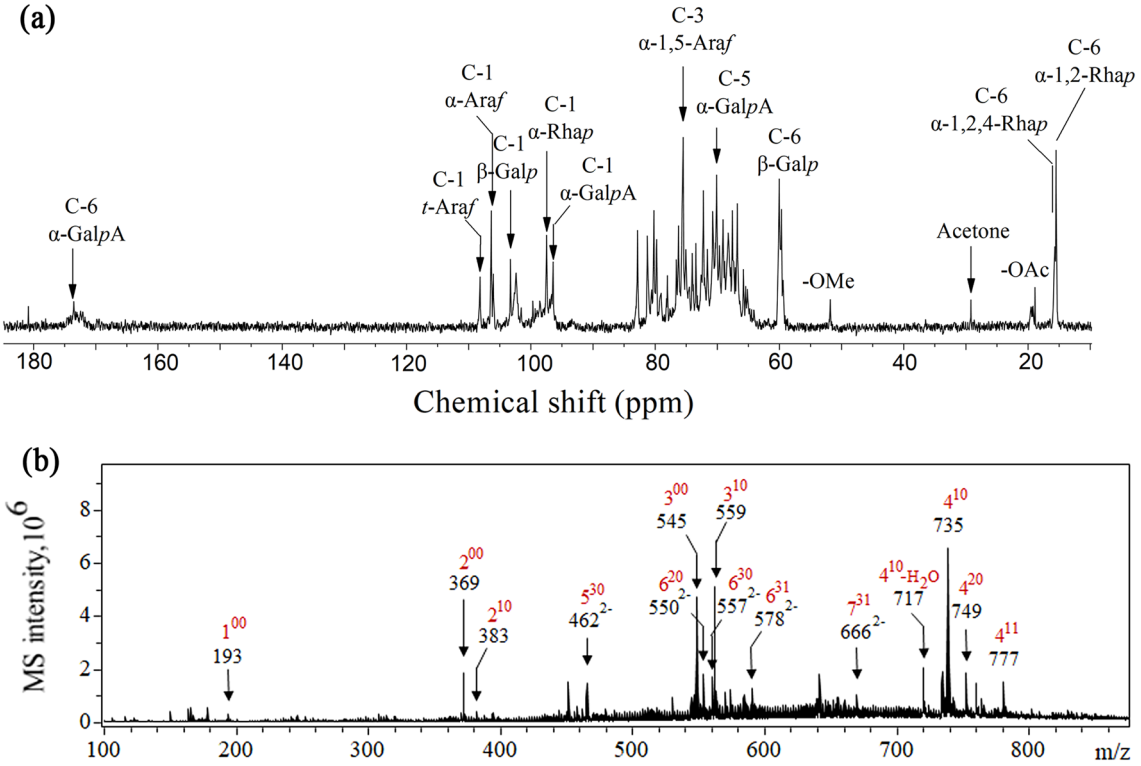

Fig. 7 **a** The ^{13}C NMR spectrum of A2c-E1. **b** ESI–MS analysis of A2c-E3. Peak annotation: e.g. 6^{31} means DP 6 with 3 methyl ester groups and 1 acetyl group

Table 5 Chemical shifts of the ^{13}C-NMR spectrum of A2c-E1

Fractions	Sugar Residues	Chemical Shifts, δ (ppm)					
		C-1	C-2	C-3	C-4	C-5	C-6
A2c-E1	→4)-α-Gal*p*A-(1→	96.40	67.10	68.20	76.20	70.11	173.57
	→2)-α-Rha*p*-(1→	97.48	75.68	69.10	71.67	70.76	15.52
	→2,4)-α-Rha*p*-(1→	97.48	75.68	69.10	74.05	70.76	15.75
	→4)-β-Gal*p*-(1→	103.96	71.67	73.21	77.62	74.47	59.70
	t-β-Gal*p*-(1→	103.29	71.61	72.25	–	73.43	60.09
	→3)-β-Gal*p*-(1→	102.38	71.61	79.01	68.23	74.86	59.85
	→6)-β-Gal*p*-(1→	102.38	71.61	72.25	68.23	74.86	67.37
	→3,6)-β-Gal*p*-(1→	101.59	71.61	79.01	68.23	74.86	67.37
	→5)-α-Ara*f*-(1→	106.35	81.24	75.47	82.86	65.45	–
	→3,5)-α-Ara*f*-(1→	106.01	79.73	82.59	82.86	65.45	–
	t-α-Ara*f*-(1→	108.20	81.24	75.66	82.86	60.05	–

However, until now, the detailed structural features of the polysaccharides from *Hedera nepalensis* have remained unknown. Therefore, in this paper, water-soluble polysaccharides from *Hedera nepalensis* were systematically fractionated and characterized.

Total polysaccharide (WHNP) was fractionated into neutral and acidic polysaccharides by using anion-exchange chromatography, respectively. It was found that the yield of neutral polysaccharide (WHNP-N, yield 72.0%) was higher than that of acidic polysaccharide (WHNP-A, yield 15.1%), respectively. Monosaccharide composition indicated that WHNP-N was mainly composed of Glc (47.9%), Gal (22.0%) and Ara (11.6%). In this study, the neutral polysaccharide fraction WHNP-N was

not further analyzed. Based on the charge distribution homogeneity analyses, WHNP-A exhibited an inhomogeneous charge distribution. As a result, it was further fractionated by using anion-exchange chromatography and Sepharose CL-6B column, obtaining three major pectin fractions (WHNP-A2b, WHNP-A2c and WHNP-A3b). Then, the structural features of these major pectin fractions were further analyzed.

Monosaccharide composition indicated that WHNP-A2b, WHNP-A2c and WHNP-A3b were mainly composed of GalA, Rha, Gal and Ara residues, especially, and WHNP-A2c contained GalA (60.8%) as the major sugar. Also, based on FT-IR analysis, the DM of WHNP-A2c was 24.4%, higher than those of WHNP-A2b (15.5%) and WHNP-A3b (6.1%). From the monosaccharide composition, TBA, NMR and methylation analyses, it could be found that both WHNP-A2b and WHNP-A3b predominantly contained RG-I domains, while WHNP-A2c mainly consisted of RG-I, RG-II and HG domains. According to the NMR and methylation analyses, it could be expected that the WHNP-A2b mainly contained α-L-1,5/1,3,5-arabinan, AG-II, β-D-1,4-galactan and/or AG-I as side chains, whereas WHNP-A3b predominantly contained β-D-1,4-galactan, α-L-1,5/1,3,5-arabinan and AG-II as side chains. Also, in WHNP-A2c, RG-I domain (A2c-E1), RG-II domain (A2c-E2) and oligosaccharide (A2c-E3) were fractionated by using endo-PG hydrolysis and size-exclusion chromatography with the mass ratios of 1.8:1.0:0.6, indicating that this fraction mainly contained RG-I-type domain. NMR and methylation analyses revealed that RG-I-type domain (A2c-E1) mainly contained α-L-1,5/1,3,5-arabinan, AG-II, β-D-1,4-galactan and/or AG-I as side chains, and the neutral side chains might be short. Besides, ESI–MS analysis showed that the HG-type pectin oligosaccharides (A2c-E3) encompassed a wide range of GalA oligomers from DP 1 to DP 7.

In previous studies, similar studies have been reported for pectic polysaccharides obtained from other medicinal plants, such as *Panax notoginseng* [33], *Isatis indigotica* Fort. [30] and Radix *Sophorae Tonkinensis* [20], which fractionated and structurally characterized RG-I, RG-II, and HG domains using Endo-PG. However, these had differences in the mass ratios of RG-I, RG-II and HG domains and structural features. Also, it has been reported that pectic polysaccharides obtained from various plant sources such as Radix *Sophorae Tonkinensis* (20), *Isatis indigotica* Fort. [30], *Panax notoginseng* [33], *Saussurea involucrata* [45] and *Codonopsis pilosula* [46] and *Ziziphus jujube* [47, 48] as well as *Hedera nepalensis* contained α-L-1,5-arabinan, α-L-1,3-arabinan, α-L-1,3,5-arabinan, β-D-1,4-galactan or/ and AG-I and AG-II as side chains. However, these pectins differ in terms of molecular weights, side chain lengths and other structural characteristics [20, 30, 33, 47, 48].

Many studies have reported that some pectic polysaccharides obtained from other herbal medicines, which contained α-L-1,5/1,3,5-arabinan, β-D-1,4-galactan and/or AG-I and AG-II as side chains, possess anti-oxidant activities [20, 48–50]. In this paper, WHNP-A2b and WHNP-A3b primarily contained RG-I domains, while WHNP-A2c was mainly composed of RG-I, RG-II and HG domains. It has been reported that pectic fractions, which possess higher content of GalA residues, display stronger antioxidant activity in scavenging different radicals, and exhibit a dose response relationship [20, 48–50]. Therefore, WHNP-A3b might show stronger anti-oxidant activity than WHNP-A2b as WHNP-A3b contained more GalA than WHNP-A2b. Also, it was reported that pectic fractions, which mainly contained HG, RG-II and RG-I domains, exhibited antioxidant activity via apparent synergism from its different pectin domains, with HG domains displaying the greatest activity [20, 50]. Based on these reports, WHNP-A2c might display antioxidant activities with synergistic effects from different domains, with A2c-E3 fraction (HG domains) displaying superior activity compared to A2c-E2 (RG-II domains) and A2c-E1 (RG-I domains) fractions. Therefore, WHNP-A2b, WHNP-A2c and WHNP-A3b characterized in this paper, might correlate with antioxidant activities, and we speculated that these pectins could be used as the natural antioxidant agent.

Conclusion

In this paper, water-soluble polysaccharides isolated from the dried leaves of *Hedera nepalensis* were systematically fractionated into one neutral fraction and three major pectin fractions (WHNP-A2b, WHNP-A2c and WHNP-A3b). The chemical structures of these major pectin fractions were analyzed and compared using the sugar composition, TBA assay, FT-IR, NMR, enzymatic and methylation analyses. Results showed that WHNP-A2b and WHNP-A3b mainly contained RG-type pectins, whereas WHNP-A2c was primarily composed of RG-I, RG-II and HG domains, with mass ratios of 1.8:1.0:0.6. In WHNP-A2b and WHNP-A2c, RG-I domains primarily substituted with α-L-1,5/1,3,5-arabinan, AG-II, β-D-1,4-galactan and/or AG-I side chains. Also, in WHNP-A3b, the RG-I domains mainly contained α-L-1,5/1,3,5-arabinan, β-D-1,4-galactan and AG-II as side chains. HG domains in WHNP-A2c were degraded into oligogalacturonides with DP 1–7, carrying less than 3 methyl-esterified groups and/or 1 acetyl-esterified group. The results provide useful structural information on the polysaccharides from the dried leaves of *Hedera nepalensis*, which

will contribute to further studies of their structure–activity relationships.

Supplementary Information

The online version contains supplementary material available at https://doi.org/10.1186/s40538-023-00427-2.

Additional file 1: Figure S1. Ultraviolet spectra of **a** WHNP-A2b, **b** WHNP-A2c and **c** WHNP-A3b. **Figure S2.** GC elution profile of PMAAs derived from **a** WHNP-A2b, **b** WHNP-A2c, **c** WHNP-A3b and **d** A2c-E1.

Acknowledgements
Not applicable.

Author contributions
Investigation, Writing-original draft preparation, CHH; Investigation, YW; Formal analysis, XL; Supervision, Modify the manuscript, YZ; Writing-review & editing, UHP; Supervision, Writing-review & editing, LS. All authors contributed to the article and approved the submitted version.

Funding
This work was supported by the Scientific and Technologic Foundation of Jilin Province (20200201154JC), National Natural Science Foundation of China (32271339), Fundamental Research Funds for the Central Universities (CGZH202206) and Innovation Platform Project of Qinghai province (2021-ZJ-T02).

Declarations

Ethics approval and consent to participate
All methods were performed in accordance with the relevant guidelines and regulations.

Consent for publication
Not applicable.

Competing interests
The authors declare that they have no known competing financial interests or personal relationships that could have appeared to influence the work reported in this paper.

Author details
[1]Engineering Research Center of Glycoconjugates of Ministry of Education, Jilin Provincial Key Laboratory On Chemistry and Biology of Changbai Mountain Natural Drugs, School of Life Sciences, Northeast Normal University, Changchun 130024, China.

Received: 29 May 2023 Accepted: 5 June 2023
Published online: 12 June 2023

References

1. Saleem S, Jafri L, Haq I, Chang L, Calderwood D, Green BD, Mirza B. Plants *Fagonia cretica* L. and Hedera nepalensis K Koch contain natural compounds with potent dipeptidyl peptidase-4 (DPP-4) inhibitory activity. J Ethnopharmacol. 2014;156:26–32. https://doi.org/10.1016/j.jep.2014.08.017.
2. Wu J, Zhou X, Gao J, Peng Y, Hu S, Qian Y, Zhang C, Wang RH, Qi ZC. The complete chloroplast genome sequence of common Chinese ivy *Hedera nepalensis* var. sinensis (Araliaceae). Mitochondrial DNA Part B. 2019;4:1881–2. https://doi.org/10.1080/23802359.2019.1591201.
3. Hashmi WJ, Isamail H, Mehmood F, Mirza B. Neuroprotective, antidiabetic and antioxidant effect of *Hedera nepalensis* and lupeol against STZ + $AlCl_3$ induced rats model. Daru J Pharm Sci. 2018;26:179–90. https://doi.org/10.1007/s40199-018-0223-3.
4. Hashmi WJ, Isamail H, Jafri L, Mirza B. Ethnopharmacological activity of Hedera nepalensis K. Koch extracts and lupeol against alloxan-induced type I diabetes. Braz J Pharm Sci. 2020;56:1–15. https://doi.org/10.1590/s2175-97902019000318406.
5. Asif M, Zafar M, Saleem M, Saadullah M, Khalid SH, Khan MSS, Mahruks IZ, Khan IU, Hussain L, Yaseen HS, Zubair M. Evaluation of antidiabetic and wound healing properties of ethanol extract of *Hedera nepalensis* in alloxan-induced diabetic rats. S Afr J Bot. 2022;146:118–26. https://doi.org/10.1016/j.sajb.2021.10.007.
6. Ahmad B, Munir N, Bashir S, Azam S, Khan I, Ayub M. Biological screening of *Hedera nepalensis*. J Med Plants Res. 2012;6:5250–7. https://doi.org/10.5897/JMPR12.244.
7. Li T, Pan H, Feng Y, Li H, Zhao Y. Bioactivity-guided isolation of anticancer constituents from *Hedera nepalensis* K. Koch S Afr J Bot. 2015;100:87–93. https://doi.org/10.1016/j.sajb.2015.05.011.
8. Jafri L, Saleem S, Kondrytuk TP, Haq I, Ullah N, Pezzuto JM, Mirza B. Hedera nepalensis K Koch: a novel source of natural cancer chemopreventive and anticancerous compounds. Phytother Res. 2016;30:447–53. https://doi.org/10.1002/ptr.5546.
9. Jafri L, Saleem S, Haq I, Ullah N, Mirza B. *In vitro* assessment of antioxidant potential and determination of polyphenolic compounds of *Hedera nepalensis* K. Koch Arab J Chem. 2017;10:S3699–706. https://doi.org/10.1016/j.arabjc.2014.05.002.
10. Duong HT, Trieu LH, Linh DTT, Duy LX, Thao LQ, Van Minh L, Hiep NT, Khoi NM. Optimization of subcritical fluid extraction for total saponins from *hedera nepalensis* leaves using response surface methodology and evaluation of its potential antimicrobial activity. Processes. 2022;10:1268. https://doi.org/10.3390/pr10071268.
11. Kizu H, Kitayama S, Nakatani F, Tomimori T, Namba T. Studies on Nepalese Crude Drugs. III.1) On the Saponins of Hedera nepalensis K KOCH2). Chem Param Bull. 1985;33:3324–9. https://doi.org/10.1248/cpb.33.3324.
12. Zhang X, Li S, Sun L, Ji L, Zhu J, Fan Y, Tai GH, Zhou YF. Further analysis of the structure and immunological activity of an RG-I type pectin from *Panax ginseng*. Carbohydr Polym. 2012;89:519–25. https://doi.org/10.1016/j.carbpol.2012.03.039.
13. Cheng H, Zhang Z, Leng J, Liu D, Hao M, Gao X, Tai GH, Zhou YF. The inhibitory effects and mechanisms of rhamnogalacturonan I pectin from potato on HT-29 colon cancer cell proliferation and cell cycle progression. Int J Food Sci Nutr. 2013;64:36–43. https://doi.org/10.3109/09637486.2012.694853.
14. Wang D, Wang C, Li J, Zhao G. Components and activity of polysaccharides from coarse tea. J Agric Food Chem. 2001;49:507–10. https://doi.org/10.1021/jf000029m.
15. Yang X, Liu H, Yang J, Ma Z, Guo P, Chen H, Gao D. Purification, structural characterization and immunological activity of *Sibiraea laexigata* (L.) Maxim polysaccharide. Front Nutr. 2022;9:1013020. https://doi.org/10.3389/fnut.2022.1013020.
16. Dubois M, Gilles KA, Hamilton JK, Rebers PA, Smith F. Colorimetric Method for Determination of Sugars and Related Substances. Anal Chem. 1956;28:350–6. https://doi.org/10.1021/ac60111a017.
17. Blumenkrantz N, Asboe-Hansen G. New method for quantitative determination of uronic acids. Anal Biochem. 1973;54:484–9. https://doi.org/10.1016/0003-2697(73)90377-1.
18. Zhang X, Yu L, Bi H, Li X, Ni W, Han H, Li N, Wang B, Zhou Y, Tai G. Total fractionation and characterization of the water-soluble polysaccharides isolated from *Panax ginseng C*. A Meyer Carbohydr Polym. 2009;77:544–52. https://doi.org/10.1016/j.carbpol.2009.01.03.
19. York WT, Darvill AG, McNeil M, Albersheim P. 3-deoxy-d-*manno*-2-octulosonic acid (KDO) is a component of rhamnogalacturonan II, a pectic polysaccharide in the primary cell walls of plants. Carbohydr Res. 1985;138:109–26. https://doi.org/10.1016/0008-6215(85)85228-9.
20. Ning X, Liu Y, Jia M, Wang Q, Sun Z, Ji L, Mayo KH, Zhou Y, Sun L. Pectic polysaccharides from Radix *Sophorae Tonkinensis* exhibit significant antioxidant effects. Carbohydr Polym. 2021;262:117925. https://doi.org/10.1016/j.carbpol.2021.117925.
21. Pettolino FA, Walsh C, Fincher GB, Bacic A. Determining the polysaccharide composition of plant cell walls. Nat Protoc. 2012;7:1590–607. https://doi.org/10.1038/nprot.2012.081.
22. Anumula KR, Taylor PB. A comprehensive procedure for preparation of partially methylated alditol acetates from glycoprotein carbohydrates.

Anal Biochem. 1992;203:101–8. https://doi.org/10.1016/0003-2697(92)90048-C.
23. Cui L, Wang J, Huang R, Tan Y, Zhang F, Zhou Y, Sun L. Analysis of pectin from *Panax ginseng* flower buds and their binding activities to galectin-3. Int J Biol Macromol. 2019;128:459–67. https://doi.org/10.1016/j.ijbiomac.2019.01.129.
24. Chaharbaghi E, Khodaiyan F, Hosseini SS. Optimization of pectin extraction from pistachio green hull as a new source. Carbohydr Polym. 2017;173:107–13. https://doi.org/10.1016/j.carbpol.2017.05.047.
25. Manrique GD, Lajolo FM. FT-IR spectroscopy as a tool for measuring degree of methyl esterification in pectins isolated from ripening papaya fruit. Postharvest Biol Technol. 2002;25:99–107. https://doi.org/10.1016/S0925-5214(01)00160-0.
26. Singthong J, Cui SW, Ningsanond S, Douglas GH. Structural characterization, degree of esterification and some gelling properties of Krueo Ma Noy (*Cissampelos pareira*) pectin. Carbohydr Polym. 2004;58:391–400. https://doi.org/10.1016/j.carbpol.2004.07.018.
27. Zhao S, Han Z, Yang L, Hong B, Zhu H. Extraction, characterization and antioxidant activity evaluation of polysaccharides from *Smilacina japonica*. Int J Biol Macromol. 2020;151:576–83. https://doi.org/10.1016/j.ijbiomac.2020.02.015.
28. Taboada E, Fisher P, Jara R, Zúñiga E, Gidekel M, Cabrera JC, Pereira E, Gutiérrez-Moraga A, Villalonga R, Cabrera G. Isolation and characterisation of pectic substances from murta (*Ugni molinae* Turcz) fruits. Food Chem. 2010;123:669–78. https://doi.org/10.1016/j.foodchem.2010.05.030.
29. Bai X, Liu P, Shen H, Zhang Q, Zhang T, Jin X. Water-extracted *Lonicera japonica* polysaccharide attenuates allergic rhinitis by regulating NLRP3-IL-17 signaling axis. Carbohydr Polym. 2022;297:120053. https://doi.org/10.1016/j.carbpol.2022.120053.
30. Pak UH, Yu Y, Ning X, Ho CH, Ji L, Mayo KH, Zhou Y, Sun L. Comparative study of water-soluble polysaccharides isolated from leaves and roots of *Isatis indigotica* Fort. Int J Biol Macromol. 2022;206:642–52. https://doi.org/10.1016/j.ijbiomac.2022.02.187.
31. Lin L, Wang P, Du Z, Wang W, Cong Q, Zheng C, Jin C, Ding K, Shao C. Structural elucidation of a pectin from flowers of *Lonicera japonica* and its antipancreatic cancer activity. Int J Biol Macromol. 2016;88:130–7. https://doi.org/10.1016/j.ijbiomac.2016.03.025.
32. Sun L, Wu D, Ning X, Yang G, Lin Z, Tian M, Zhou Y. α-Amylase-assisted extraction of polysaccharides from *Panax ginseng*. Int J Biol Macromol. 2015;75:152–7. https://doi.org/10.1016/j.ijbiomac.2015.01.025.
33. Chan MK, Yu Y, Wulamu S, Wang Y, Wang Q, Zhou Y, Sun L. Structural analysis of water-soluble polysaccharides isolated from *Panax notoginseng*. Int J Biol Macromol. 2020;155:376–85. https://doi.org/10.1016/j.ijbiomac.2020.03.233.
34. Yu L, Zhang X, Li S, Liu X, Sun L, Liu H, Iteku J, Zhou Y, Tai GH. Rhamnogalacturonan I domains from ginseng pectin. Carbohydr Polym. 2010;79:811–7. https://doi.org/10.1016/j.carbpol.2009.08.028.
35. Catoire L, Goldberg R, Pierron M, Morvan C, Penhoat HDC. An efficient procedure for studying pectin structure which combines limited depolymerization and ^{13}C NMR. Eur Biophys J. 1998;27:127–36. https://doi.org/10.1007/s002490050118.
36. Tamiello CS, do Nascimento GE, Iacomini M, Cordeiro LMC. Arabinogalactan from edible jambo fruit induces different responses on cytokine secretion by THP-1 macrophages in the absence and presence of pro-inflammatory stimulus. Int J Biol Macromol. 2018;107:35–41. https://doi.org/10.1016/j.ijbiomac.2017.08.148.
37. Ichiyanagi T, Yamasaki R. Anomeric O-acylation of Kdo using alkyl and aryl isocyanates. Carbohydr Res. 2005;340:2682–7. https://doi.org/10.1016/j.carres.2005.09.002.
38. Juliane C, Lauro M, Cristiane H, Maria F, Daniele M, Guilherme L, Marcello I, Thales RC. Polysaccharides from *Arctium lappa* L.: Chemical structure and biological activity. Int J Biol Macromol. 2016;91:954–60. https://doi.org/10.1016/j.ijbiomac.2016.06.033.
39. Yu Y, Cui L, Liu X, Wang Y, Song C, Pak UH, Mayo KH, Sun L, Zhou Y. Determining Methyl-Esterification Patterns in Plant-Derived Homogalacturonan Pectins. Front Nutr. 2022;9:925050. https://doi.org/10.3389/fnut.2022.925050.
40. Wu D, Cui L, Yang G, Ning X, Sun L, Zhou Y. Preparing rhamnogalacturonan II domains from seven plant pectins using *Penicillium oxalicum* degradation and their structural comparison. Carbohydr Polym. 2018;180:209–15. https://doi.org/10.1016/j.carbpol.2017.10.037.
41. Shi H, Yu L, Shi Y, Lu J, Teng H, Zhou Y, Sun L. Structural characterization of a rhamnogalacturonan I domain from ginseng and its inhibitory effect on galectin-3. Molecules. 2017;22:1016. https://doi.org/10.3390/molecules22061016.
42. Zhang M, Zu H, Zhuang X, Yu Y, Wang Y, Zhao Z, Zhou Y. Structural analyses of the HG-type pectin from *notopterygium incisum* and its effects on galectins. Int J Biol Macromol. 2020;162:1035–43. https://doi.org/10.1016/j.ijbiomac.2020.06.216.
43. Remoroza C, Cord-Landwehr S, Leijdekkers AGM, Moerschbacher BM, Schols HA, Gruppen H. Combined HILIC-ELSD/ESI-MS^n enables the separation, identification and quantification of sugar beet pectin derived oligomers. Carbohydr Polym. 2012;90:41–8. https://doi.org/10.1016/j.carbpol.2012.04.058.
44. Ognyanov M, Remoroza C, Schols HA, Georgiev YN, Petkova NT, Krystyjan M. Structural, rheological and functional properties of galactose-rich pectic polysaccharide fraction from leek. Carbohydr Polym. 2020;229:115549. https://doi.org/10.1016/j.carbpol.2019.115549.
45. Liu G, Kamilijiang M, Abuduwaili A, Zang D, Abudukelimu N, Liu G, Yili A, Also HA. Isolation, structure elucidation, and biological activity of polysaccharides from *Saussurea involucrata*. Int J Biol Macromol. 2022;222:154–66. https://doi.org/10.1016/j.ijbiomac.2022.09.137.
46. Li LX, Chen MS, Zhang ZY, Paulsen BS, Rise F, Huang C, Feng B, Chen XF, Jia RY, Ding CB, Feng SL, Li YP, Chen YL, Huang Z, Zhao XH, Yin ZQ, Zou YF. Structural features and antioxidant activities of polysaccharides from different parts of Codonopsis pilosula var modesta (Nannf.) L. T. Shen. Front Pharmacol. 2022;13:937581. https://doi.org/10.3389/fphar.2022.937581.
47. Ji X, Cheng Y, Tian J, Zhang S, Jing Y, Shi M. Structural characterization of polysaccharide from jujube (*Ziziphus jujuba* Mill.) fruit. Chem Biol Technol Agric. 2021;8(1):54. https://doi.org/10.1186/s40538-021-00255-2.
48. Ji X, Guo J, Ding D, Gao J, Hao L, Guo X, Liu Y. Structural characterization and antioxidant activity of a novel high-molecular-weight polysaccharide from *Ziziphus Jujuba cv Muzao*. J Food Meas Charac. 2022;16:2191–200. https://doi.org/10.1007/s11694-022-01288-3.
49. Wang L, Li L, Gao J, Huang J, Yang Y, Xu Y, Liu S, Yu W. Characterization, antioxidant and immunomodulatory effects of selenized polysaccharides from dandelion roots. Carbohydr Polym. 2021;260:117796. https://doi.org/10.1016/j.carbpol.2021.117796.
50. Qi X, Yu Y, Wang X, Xu J, Wang X, Feng Z, Zhou YF, Xiao HX, Sun L. Structural characterization and anti-oxidation activity evaluation of pectin from *Lonicera japonica* Thunb. Front Nutr. 2022;9:998462. https://doi.org/10.3389/fnut.2022.998462.

Publisher's Note